PAPER • OPEN ACCESS

Design of MoS_2/graphene heterostructure thin film sensors for high performance NO_2 gas sensor applications

To cite this article: R Sakthivel *et al* 2021 *J. Phys.: Conf. Ser.* **2070** 012131

View the article online for updates and enhancements.

Design of MoS₂/graphene heterostructure thin film sensors for high performance NO₂ gas sensor applications

R Sakthivel[1], A Geetha [2], B A Anandh[1], V Jagadeesan[1], A Shankar Ganesh[1], J Dineshkumar[3*]

[1] Department of Electronics, PSG College of Arts & Science, Civil Aerodrome Post, Coimbatore- 641 014, Tamilnadu, India.
[2]Department of Chemistry, Hindusthan College of Arts and Science, Hindusthan Gardens(Behind Nava India), Avinashi Road, Coimbatore- 641 028, Tamil Nadu, India.
[3]Department of Electrical and Communication Systems, VLB Janakiammal College of Artsand Science, Kovaipudur, Coimbatore - 641 042, Tamil Nadu, India.

Abstract. In this paper, we fabricate a large-area chemiresitive type MoS₂/graphene films sensor is grown by spray pyrolysis technique. The prepared sensor films were characterization by XRD, SEM, TEM Raman and BET analysis. The synergistic effect between MoS₂ and graphene through the CVD method produces such a hierarchical layer-by-layer assembly of the thin film structure. MoS₂/graphene hybrid films not only show enhanced NO₂ sensitivity compared to NO₂ sensitivity alone. Graphene or MoS₂ films, but they also exhibit characteristics of rapid response and strong reproducibility. Selectiveness and stability findings demonstrate the outstanding sensing properties of the MoS₂ thin film sensor. The MoS₂/G showed higher sensitivity (81%) towards NO₂ gas at the concentration of 1000 ppm followed by graphene (22 %) and MoS₂ (45 %) based sensors in sequence. The MoS₂/G sensor also exhibits fast response (12 s) and recovery time (17 s) than other sensor samples. The concept of operation and sensing mechanism behind their impressive results has also been studied in depth. The effect of humidity on the performance of gas sensing was also discussed in the point of practical device applications.

1. Introduction

Gas sensors are crucial for pollution control and air quality detection. The substances, sensing mechanism, and external influences all have an impact on a gas sensor's gas detecting capability (temperature, humidity). Due to the ability to swiftly detect hazardous gases and organic vapours for human and environmental security, emissions reduction, employment market, and medical diagnostics, gas sensing is becoming increasingly essential in modern society. Polythiophene [1–3], carbon nanotubes [4,5], and metal oxides [6,7] have all been employed to detect target gases in various forms (thick or thin films, nanorods, nanowires, etc.). Metal oxides, in instance, have a wide range of properties. Furthermore, they are frequently utilised in gas sensing because to their inexpensive cost and simplicity of manufacture.

Gadgets. Nevertheless, resistive metal oxide-based gas sensors often operate at high (more than 100 degrees Celsius), resulting in excessive power consumption and drifts in gas detecting outputs owing

to metal oxide grain development. The lack of discrimination of metal oxide-based gas sensors is yet another disadvantage [8–10]. While conductive polyesters gas sensors may operate at room temperature (RT), their detecting characteristics are influenced by air temperature, and storage in air can result in deterioration. As a result, the gas sensing industry is focusing its efforts on developing novel materials that can detect gasses at room temperature (RT), under typical ambient circumstances, and with excellent selectivity and stability [11-18]. For historical and reliable detection of environmental and ecological conditions, deformable gas sensors that can be deployed on the soil or hard surfaces to detect various gaseous compounds are important [19-25]. Nitrogen dioxide (NO_2), for example, a popular poisonous fumes created by the oxidation of NO and N_2O released from gasoline engines, often contributes to undesirable pulmonary health problems such as ulcerative colitis, alzheimers and irritation. 10-20 parts per million (ppm) of NO_2 is reported to be moderately irritating, and sensitivity to 150 ppm or greater can result in death from cerebral edema or bronchospasm. Therefore, wearable NO_2 gas sensors must be established to constantly quantify the presence of NO_2 around humans, particularly those living in urban areas with high NO_2 concentrations. With the aid of nanostructure with transition metal dichalcogenides (TMDs) as a suitable sensing materials in the field of high performance gas sensors due to its suitable electronic configuration, high electrical conductivity with specific surface area.

Among various TMDs, molybdenum disulfide (MoS_2) has considered being a successful candidate for materials that detect various toxic and hazardous gases, which is present in our environment. The MoS_2-based gas sensors mentioned, however, have typically struggled from many issues, such as low sensitivity, lengthy time to react and poor recovery. In addition, an inert atmosphere was generally required for the identification of gases due to the MoS_2 has low stabilization and selectivity. Recent attempts have been made to combine MoS_2 with other materials, such as semiconducting metals, oxide based nanostructures and polymers to enhancing the sensing performance. Graphene/MoS_2 hybrids have recently been produced and have shown better performance in field of lithium ion batteries, supercapcitors, photodetectors and field-effect transistors (FETs), etc. In general, the excellent efficiency of MoS_2/graphene hybrids was due to the beneficial charge transport through the framework of the heterojunction. Such electronic structure mediated by band energy synchronization has been shown to be successful in improving the efficiency of gas sensing in hybrid materials. Nevertheless, little research has been published on the use of graphene/MoS_2 hybrids for room- temperature gas sensors. Herein, we report on a CVD assisted ultra thin with porous MoS_2/graphene hybrid thin film sensor for detection of NO_2 gas. The results showed the MoS_2/graphene hybrid sensor to demonstrate a remarkable reaction/recovery against NO_2 gas with high stability and repeatability than compared with other target gases like H_2, NH_3, SO_2, and CO_2 etc. the sensing performance of the sensor was also monitored with the presence the various humidity level (10-90%) in the point of practical device applications.

2. Experimental

2.1. Fabrication of MoS₂ and MoS₂/graphene thin films

Based on the previous literature work, the bare graphene was synthesized from graphite powder using a hydrothermal method [26]. The fluorine doped tin oxide (FTO) glass substrate was cut in 2 x 2 cm and washed with ethanol, and water finally ultrasonicated for 30 min. In the hydrothermal process, 0.5 g of $MoCl_2$ and 1 g of thiourea was dissolved in 50 mL of DI water. Then 10 mL of NaOH was added slowly in the above mixture and set the pH value of 8. A 1.7MHz ultrasonic oscillator commodified the solution, and the resulting spray was transported directly to the warmed substrate using pressurized water as a carrier gas at a flow rate of 5 L/min. Six spray cycles were chosen as the optimum location. After that, the formed FTO substrate was removed and processed in a dessicator for 24 hours at a low vacuum (about 10^2 mbar). The as synthesized films were named as pure MoS_2. In MoS_2/graphene film, 0.5 g of graphite powder was mixed with MoS_2 precursor solution then same spray pyrolysis method was carried out. Finally, the dried FTO film was named as MoS_2/graphene film.

2.2. Fabrication of gas sensor set up

The experimental setup to describe the gas sensor provided is shown in figure 1. The major aspect is the metal chamber which has the supply for the gas inlet and outlet. Using a rubber septum, the chamber is kept airtight. The vacuum was generated from inside chamber by using the rotary pump connected to it before the measurements began. For the regulation of gas flow rate and gas mixed concentration, mass flow controllers (MFC) were used. In order to obtain a given gas concentration, a specific amount of O_2 was then pumped into the mixing chamber and transported to the test chamber. Gas concentrations were adjusted from 100 to 1000 ppm and the sensing response was recorded using the Keithley 4200 digital meter.
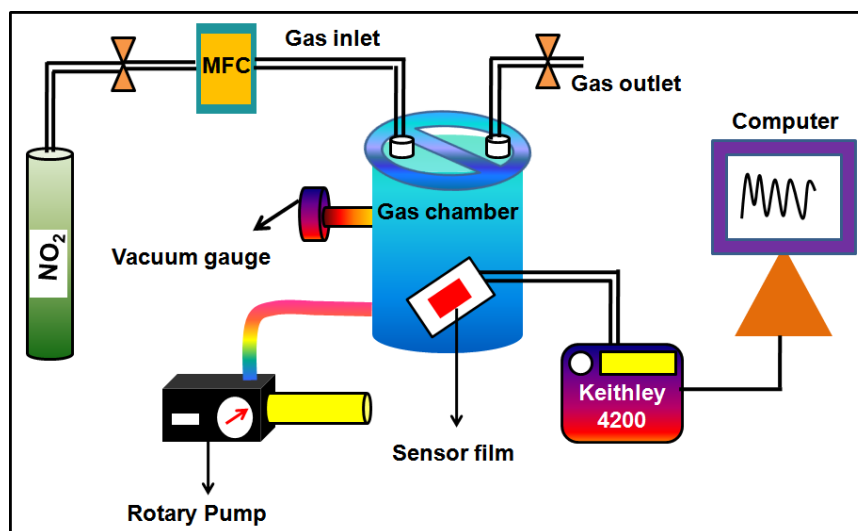
Figure 1. Schematic representation of the resistive type gas sensor setup

3. Results and discussion

3.1. Structural studies

The structural properties of graphene, MoS_2, and MoS_2/G films were identified by XRD and the spectra is depicts in Figure 2. The peak at 26.97°, corresponds to the d-spacing of 0.38 nm is due to (002) plane of graphene [27]. The pattern identified from MoS2 is belongs to hexagonal crystal structure and the reflected planes of (002), (100), (103), (105) and (110) are good accordance with the standard data (JCPDS card no. 37-1492). The (002) plane of graphene present along with all the MoS_2 related plane in the MoS_2/G composite sample. This could be explaining that the graphene was incorporated in to MoS_2 crystalline structure. There is no evident in any impurities, which suggest that product purity of the fabricate films. The successful hybridization of graphene in to MoS_2 and its structural perfection of the films were further analyzed using Raman spectra and the corresponding plot is shown in Figure 3. The Raman intense peaks were situated at 1356 cm^{-1} and 1553 cm^{-1} in the bare graphene, which is arises from the D and G bands of carbon [28]. Moreover, the calculated I_D/I_G value is close to 1.28, which implying that graphene was highly disorder. The E_{2g} and A_{1g} Raman modes of hexagonal structure MoS_2 [29], which is positioned at the relative wavenumber of 375 cm^{-1} and 411 cm^{-1}, respectively.

3.2. Morphological studies

SEM and TEM were performed to identify the morphology characteristics of the films. Figure 4 (a-c) shows the SEM images of graphene, MoS_2 and MoS_2/G composite films, respectively. The clear uniform and compact sheet like morphology was observed in the pristine graphene (Fig. 4a). The granular nano-level grains of MoS_2 (Fig. 4b), which is uniformly decorated on the graphene nanosheets surface in the MoS_2/G composite film sample (Fig. 4c).
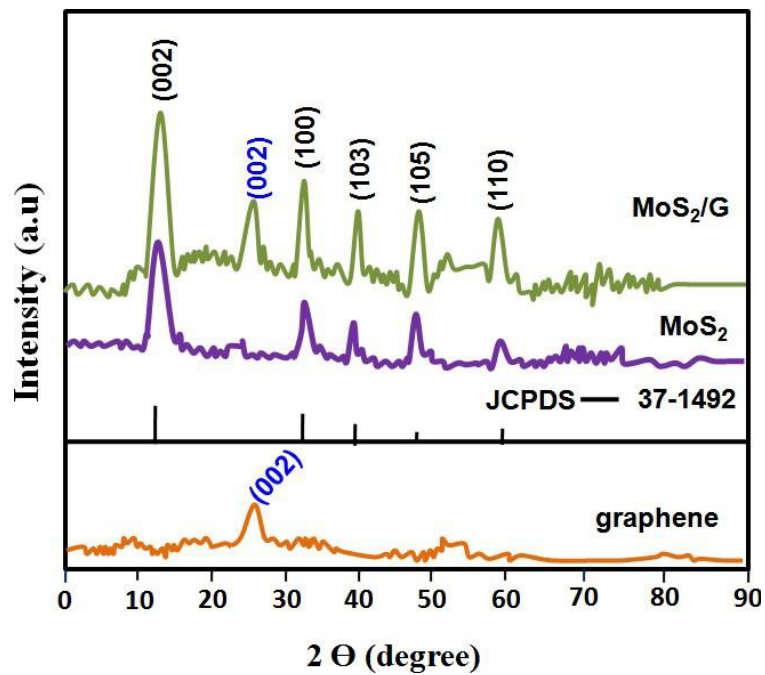
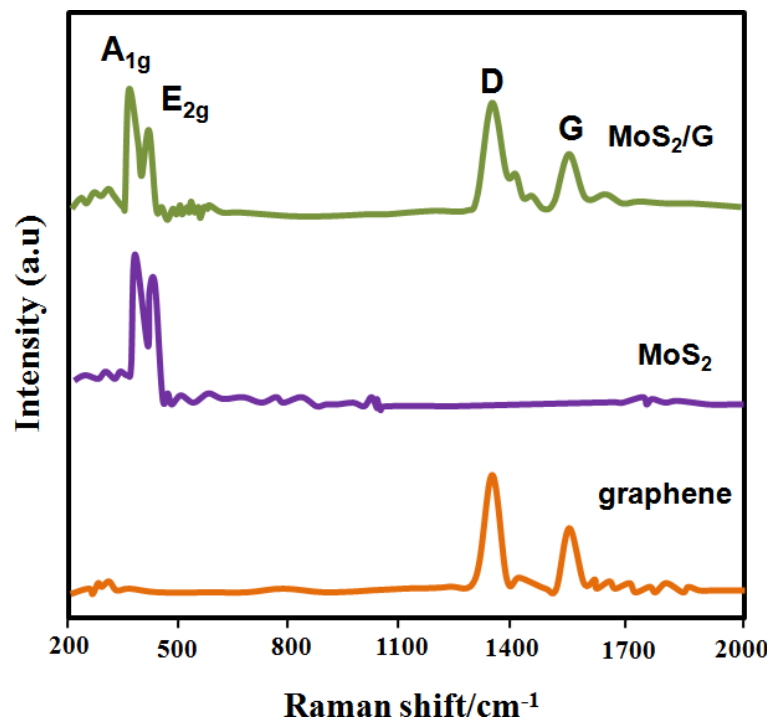**Figure 2.** X-ray diffraction pattern of the sensor samples

**Figure 2.** Raman spectra of the sensor samples

The TEM images of graphene and MoS_2 clearly exhibits layer type sheets (diameter in several micrometers) and nanoparticles with sizein the range of 20-30 nm were noticed. In MoS_2/G composite film, the MoS_2 nano-crystallites are attached on the graphene sheet surface uniformly (Fig. 4f). The HRTEM image of MoS_2 shows clear lattice fringes of 0.267 nm belonging to (002) plane of MoS_2 (Fig. 4g).

The existence of Mo, S and C elements in the MoS_2/G composite film EDS image (Fig. 4h) was additional proof to graphene wassuccessfully exploited in the MoS_2 crystal frame work.
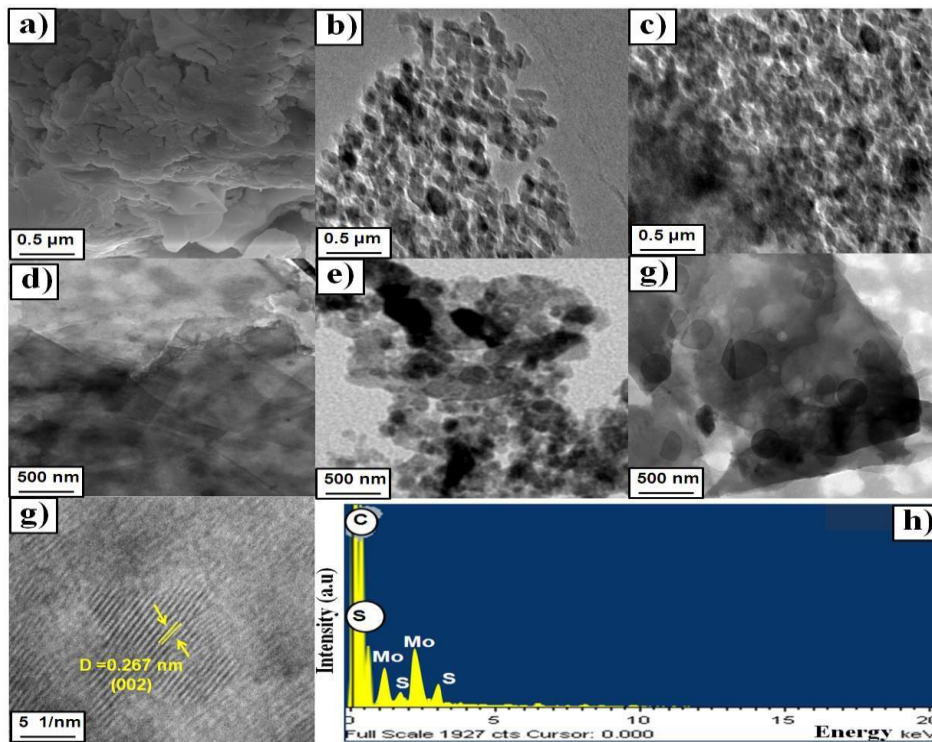
Fig.4. SEM images of **a)** graphene; **b)** MoS_2; **c)** MoS_2/G; TEM images of **d)** graphene; **e)** MoS_2; **f)** MoS_2/G; **g)** HRTEM of MoS_2/G and **h)** EDS of MoS_2/G

3.3. Surface area analysis
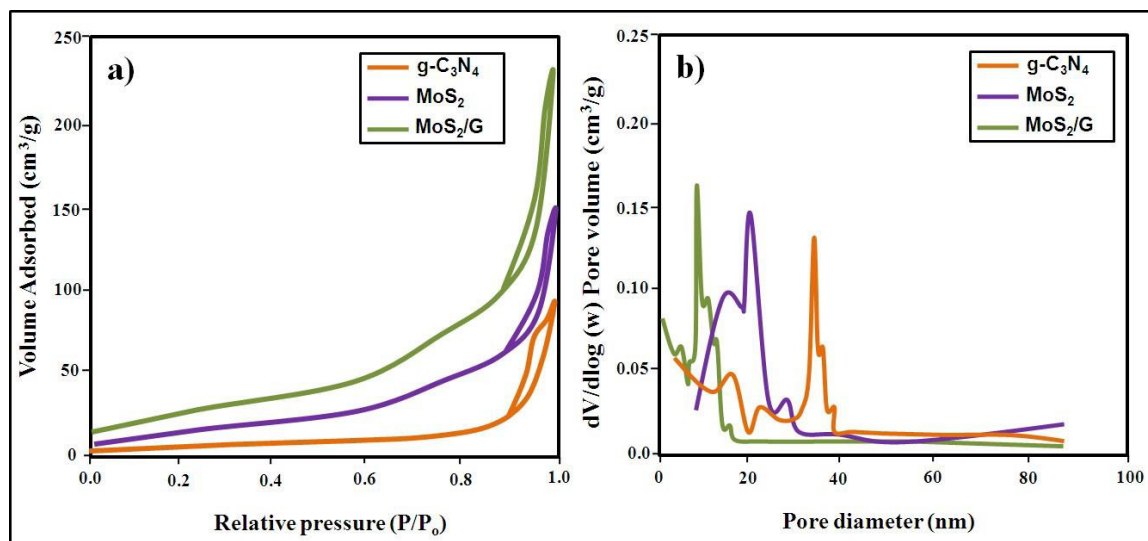
Figure 5. a) N_2 adsorption and desorption analysis of graphene, MoS_2, MoS_2/G and **b)** corresponding pore size distribution

The gas sensing features of nanostructured materials are closely link to the surface area and porosity available. Hence, N_2 adsorption-desorption isotherms were studied to identify precise surface area and porosity of graphene, MoS_2 and MoS_2/G films, respectively.   Fig. 5 shows the isotherms of all the films, which demonstrates that hysteresis loop type IV isotherms. These findings suggest that the pore volumes in these samples are delivered by mesoporous [30-32], thus ensuring adequate efficient transportation channels. MoS_2/G composite films deliver a high surface area (91.3 m^2/g) and pore diameter (8.5 nm) than compared to pure graphene (24.5 m^2/g and 36.8 nm) and MoS_2 (37.8 m^2/g and 23.8 nm).
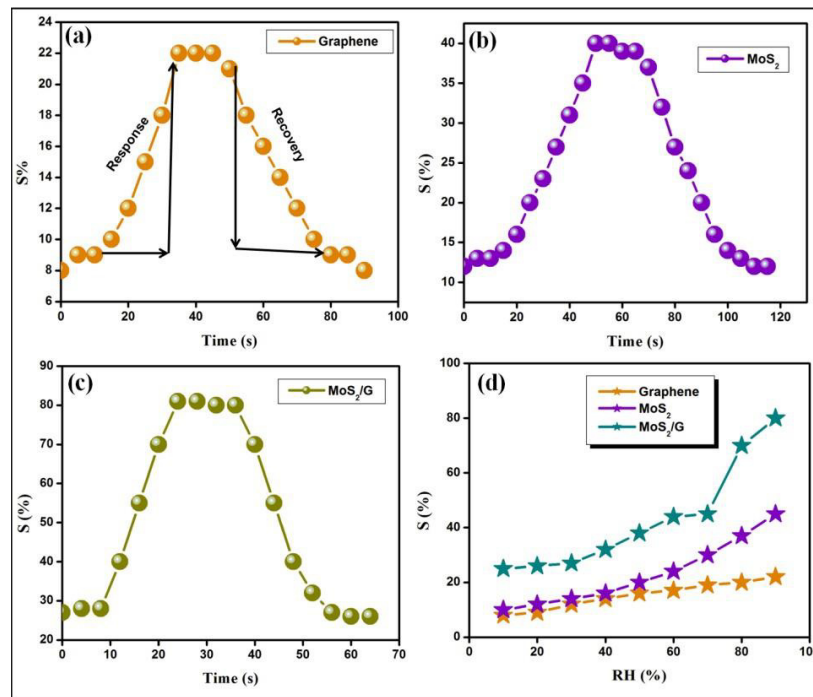
3.4. Gas sensing test

Before testing the gas sensing, the sensor films were expose to air atmosphere to check the resistance behavior of the samples. The resistance nature of the sensor was analyzed as a function of temperature and the resultant graph is displayed in Figure 6 (a). As shown in Figure the resistance of films was gradually increases with increase of temperature.
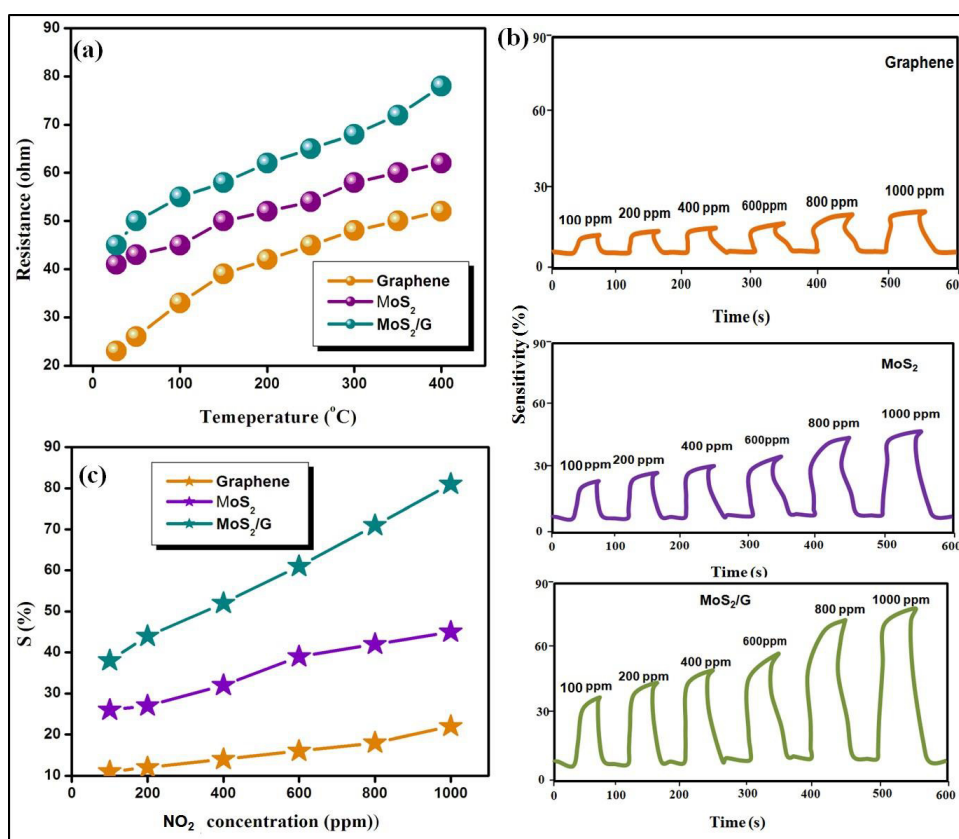

Figure 6. a) Resistance variation as a function of temperature; **b)** Dynamic response of NO_2 gas and **c)** sensitivity plot of all the sensor sample

The MoS_2/G composite film sensor shows high resistance behavior than compared to other sensors. The improved resistance nature of the composite sample is due to MoS_2 access the free electron from graphene on its surface of the films. In the NO_2 gas sensing performance different concentration (100-1000 ppm) NO_2 gas switched to the testing chamber with the help of MFC. The dynamic response of the sensor films towards H_2 gas is shown in Figure 6 (b). The sensing response of all the sensors increases with the increase of H_2 gas concentration. The sensitivity of the sensor films was defined as; $S\% = R_A/R_G/R_A \times 100\%$ [33]. The sensitivity plot of the sensor films were depicts in Figure 6 (c). The MoS_2/G showed higher sensitivity (81%) towards NO_2 gas at the concentration of 1000 ppm followed by graphene (22 %) and MoS_2 (45 %) based sensors in sequence.

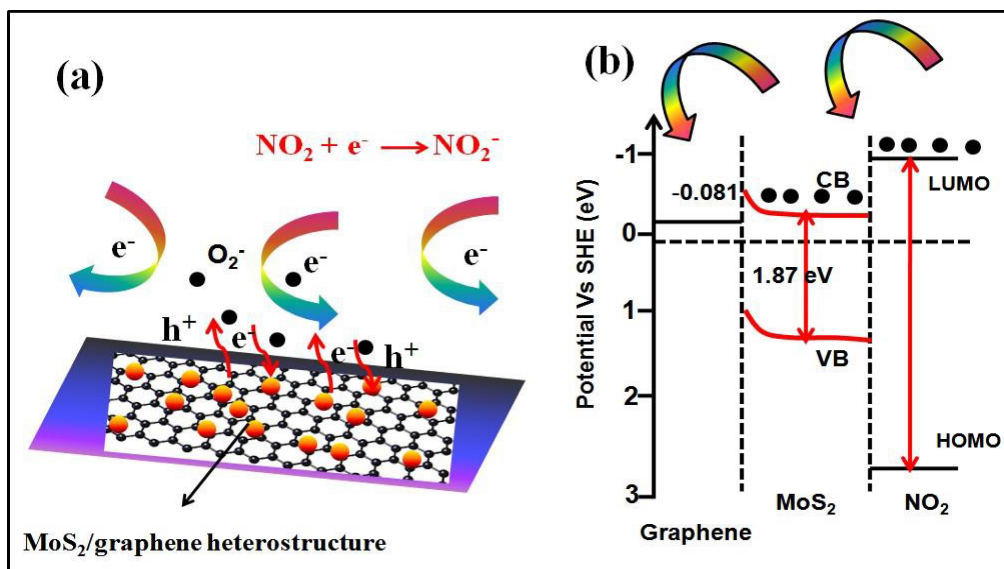**Fig.7.** Response and recovery time of **a)** graphene; **b)** MoS_2; **c)** MoS_2/G; **d)** Sensing response as a function of humidity
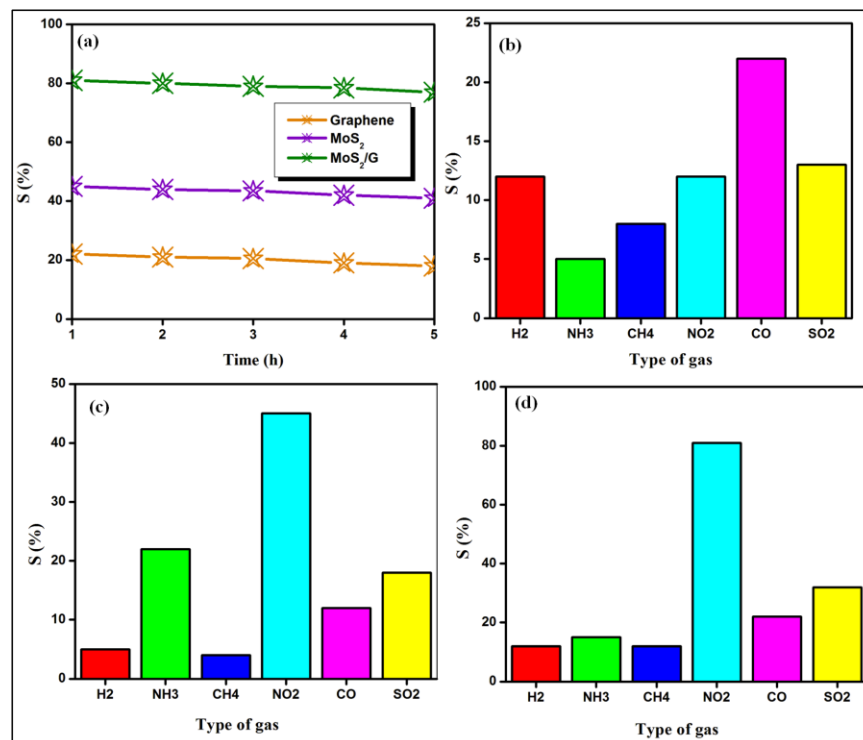
Figure 8. a) Long term stability; Selectivity response curve of **b)** graphene; **c)** MoS_2; **d)** MoS_2/G

Figure 9. Gas sensing mechanism diagram of the MoS_2/Graphene sensor towards NO_2 gas.

We achieved the maximum sensitivity for MoS_2 after hybridization of graphene. Response (the device attain the 90% of the resistance) and recovery time (the resistance fall 90% from its original value) is key role in analyze of gas sensing. The relative graph is shown in Figure 7 (a-c). Hence, we conduct the relative test for NO_2 gas with concentration of 1000 ppm at RT. The MoS_2/G sensor show fast response (12 s) and recovery time (17 s) than other sensor samples. The overall sensing parameters values are also summarize in Table 1. We also analyze the role of humidity on the sensing performance of the films and the resultant diagram is shown in Figure 7 (d). The relative humidity (RH%) is varied from 10 to 90 %. The sensing response of sensor films was improved with the increase of RH%. The sensitivity value of MoS_2/G film is 27%, 44% and 80% with corresponding humidity level of 30%, 60% and 90%, respectively. The device's long-term reliability was also measured by exposing it to multiple NO_2 cycles for nearly five hours. The findings in Fig. 8a) show that the sensitivity loss is marginal relative to the original value, indicating that the fabricated sensors are long-term stable. The selectivity response of the sensor films were also studied in order to optimize our sensor films, which is exposed to various target gases (H_2, NH_3, CH_4, CO and SO_2) measured at 1000 ppm at RT (Fig 8 b-d). Among the other gases, NO_2 has the highest response.

Table 1. Gas sensing parameters of the sensor samples

Samples	Sensitivity (%)	Response time (s)	Recovery time (s)
Graphene	22	40	45
MoS_2	45	28	32
MoS_2/G	81	12	17

4. Conclusion

We successfully synthesized heterostructure combination of MoS_2/graphene sensor film on FTO substrate by spray pyrolysis method. The sensor displays an excellent performance toward NO_2 gas at the room temperature. The MoS_2/G showed higher sensitivity (81%) towards NO_2 gas at the concentration of 1000 ppm followed by graphene (22 %) and MoS2 (45 %) based sensors in sequence. The MoS_2/G sensor also exhibits fast response (12 s) and recovery time (17 s) than other sensor samples. The relative humidity was also crucial role in the sensing performance. The fabricated sensor

show good selective response towards NO$_2$ gas than compared to other gases and also demonstrate the long term stability. Therefore, the MoS$_2$ based gas sensor system demonstrate a versatile approach for design and developing a very promising, simple and low cost sensor for detection of trace amount of NO$_2$ gas in our environment.

References

[1]   Zhang YQ, Li Z and Ling T 2017 *J. Mater. Chem. A.* **4** 8700
[2]   Liu XH, Yin PF and Kulinich SA 2017 *ACS Appl. Mater. Interfaces.* **9** 602
[3]   Liu X, Hu. M and Wang Y 2016 *J. Alloys Compd.* **685** 364.
[4]   Kumar R, Al-Dossary O and Kumar G 2015 *Nano-Micro Lett.* **7** 97.
[5]   Kida T, Nishiyama A and Hua Z 2014, *Langmuir,* **30** 2571.
[6]   Shim YS, Zhang L and Kim DH 2014 *Sens. Actuators, B,* **198** 294.
[7]   Worsley MA, Shin SJ and Merrill MD 2015 *ACS Nano,* **9** 4698.
[8]   Wu D, Lou Z and Wang Y 2017 *Nanotechnology,* **28** 435503.
[9]   Cho, SY, Kim SJ and Lee Y 2015 *ACS Nano,* **9** 9314.
[10]   Lv S and Li C 2015 *ACS Appl. Mater. Interfaces.* **7,** 13564.
[11]   Janata J, 2003 *Nat. Mater.* **2,** 19.
[12]   Miasik JJ, Hooper A, and Tofield BC 1986 *J. Chem. Soc. Faraday Trans.* **82** 1117.
[13]   Virji S, Huang RB and Weiller BH 2004 *Nano Lett.* **4** 491.
[14]   Li J, Lu Y, Ye Q and Cinke M 2003 *Nano Lett.* **3** 929.
[15]   Wang Y 2009 *J. Sens.* **2009** 493904.
[16]   Kanan SM and El-Kadri OM 2009, *Sensors.* **9** 8158.
[17]   Liu, H 2012 *Sensors,* **12** 2610.
[18]   Fine GF and Binions R 2010 *Sensors.* **10** 5469.
[19]   Ponzoni A, Baratto C and Cattabiani N 2017 *Sensors.* **17** 714.
[20]   Wang C, Yin L and Zhang L 2010 *Sensors.* **10** 2088.
[21]   Bai H 2007 *Sensors.* **7** 267.
[22]   Yoon H 2013 *Nanomaterials.* **3** 524.
[23]   Cheah R and Forsyth M 1998 *Synth. Met.* **94** 215.
[24]   Wallace PR 1947 *Phys. Rev.* **71** 622.
[25]   Novoselov KS and Geim AK 2004 *Science.* **306** 666.
[26]   Xiang Ke and Ga-zi Hao 2016 International Conference on Nanotechnology Sendai, Japan, August 22-25.
[27]   Siburian R and Sihotanh H 2020 *Oriental Journal of Chemistry,* **34** 182.
[28]   Zhang S and Zhang N 2018 *Chem. Soc. Rev.* **47** 3217.
[29]   Tan K and Yu J 2014 *J. Appl. Phys.* **116** 064305.
[30]   BoopathiRaja R and Parthibavarman M 2019 *J. Alloy. Compd.* **811** 152084.
[31]   BoopathiRaja R, Parthibavarman M and Nishara Begum A 2019 *Vacuum.* **165** 96
[32]   Parthibavarman M, Karthik M and Prabhakaran S 2018 *Vacuum.* **155** 224.
[33]   Xian Li, Jing Wang, Dan Xie and Lan Xiang 2017 *Mater. Lett.* **189** 42.